DENTAL MATERIALS 35 (2019) 298–309

Available online at www.sciencedirect.com

ScienceDirect

journal homepage: www.intl.elsevierhealth.com/journals/dema

Biomimetic regulation of dentine remineralization by amino acid *in vitro*

Yuanmei Zhang[a,*,1], *Zhejun Wang*[b,c,1], *Tao Jiang*[b,2], *Yining Wang*[b,**]

[a] *Department of Stomatology, the First Affiliated Hospital of Zhengzhou University, No.1, Jianshe East Road, Zhengzhou, China*

[b] *The State Key Laboratory Breeding Base of Basic Science of Stomatology (Hubei-MOST) & Key Laboratory of Oral Biomedicine Ministry of Education, School & Hospital of Stomatology, Wuhan University, 237# Luoyu Road, Wuhan 430079, China*

[c] *Division of Endodontics, Department of Oral Biological & Medical Sciences, Faculty of Dentistry, University of British Columbia, Vancouver, Canada*

ARTICLE INFO

Article history:
Received 11 May 2018
Received in revised form
18 November 2018
Accepted 20 November 2018

Keywords:
Bioactive glass
Aspartic amino
Dentine remineralization

ABSTRACT

Objective. The aim of this study was to evaluate the effect of conditioning solutions containing DL-aspartic amino (Asp) on dentine remineralization induced by bioactive glass 45S5 (BAG) in a simulated oral environment.

Methods. Sixty dentine discs from human third molars were used. Dentine specimens were treated with ethylene diamine tetraacetic acid (EDTA) to create a partially demineralization model and randomly divided to 4 groups: Artificial saliva (AS) group, Asp group (pretreated with Asp and remineralized with distilled water), BAG group (pretreated with distilled water and remineralized by BAG), Asp-BAG group (pretreated with Asp and remineralized by BAG).

Each samples were measured at various time points, and at the end of the experiment, 6% citric acid challenge were taken. The remineralization characteristics were analyzed by using the spectroscopic data from attenuated total reflectance spectroscopy (ATR-IR) and Raman spectroscopy. The micro-morphology and structure were characterized by scanning electron microscopy (SEM) and X-ray diffraction (XRD). Dentine permeability was measured before and after each treatment to evaluate the resistance of remineralized layer to acid and simulated oral environment.

Results. Both BAG and Asp-BAG groups significantly reduced dentine permeability and formed enamel-like apatite layers on dentine surface. For the mineralization of BAG, Asp showed inhibition effect. The 7-day mineral matrix area ratio in BAG group (12.54 ± 2.29) was lower than the value in the Asp-BAG group (17.77 ± 2.27) ($p < 0.05$) and the Raman intensity (RI%) in Asp-BAG Group (1.49 ± 0.26) was also significantly higher than that of

* *Corresponding author at*: Department of Stomatoltgy, the First Affiliated Hospital of Zhengzhou University, No.1, Jianshe East Road, Zhengzhou, China.

** *Corresponding author at*: Department of Prosthodontics, School and Hospital of Stomotology, Wuhan University, 237# LuoYu Road, Whuhan, China.

E-mail addresses: 2013283040031@whu.edu.cn (Y. Zhang), wang.yn@whu.edu.cn (Y. Wang).

https://doi.org/10.1016/j.dental.2018.11.026

BAG group (1.34 ± 0.14) ($p < 0.05$). According to permeability test, the apatite layer in BAG group and Asp-BAG group effectively occluded the dentinal tubules ($p < 0.05$) and had certain acidic resistance ($p > 0.05$). Furthermore, adsorbed acidic amino acid on hydroxyapatite (HAP) altered the crystal to increase into a larger size in diameter during crystal growth.
Significance. The study demonstrated that a superior remineralization efficacy of BAG with Asp pretreatment on dentine.

1. Introduction

Dentine is a biological composite consisting of peculiar micro dentinal tubules [1,2]. A number of predisposing factors, for example, abrasion, erosion, gingival recession, periodontal disease and patient destructive habits may cause gingival recession and the loss of cementum or enamel, resulting in the exposure of dentinal tubules to an external environment [3,4]. Non-noxious stimuli (*e.g.* cold) may trigger fluid movement within the dentine tubules and stimulate the pulpal mechanoreceptors, ending up with a painful sensation [5–8].

Dentine hypersensitivity (DH) can be defined as a short or transient sharp pain arising from exposed dentin in response to chemical, thermal tactile, or osmotic stimuli which cannot be explained as arising from any other dental defect or disease. A recent review based on the evidence of prevalence studies reported the prevalence of DH in the population was 10% [3,5,9]. Various desensitizers such as fluoride formulations, resins and bioactive glass [10,11], have been used and demonstrated clinical efficacy for the management of DH [10–12]. Bioactive glass 45S5 (BAG) is calcium phosphosilicate cement that has been used in hard tissue repair and replacement as a osteanagenesis material in the early 1970s. Hydrolyzed BAG release calcium ions (Ca^{2+}) and phosphate ions (PO_4^{3-}) to from calcium phosphate rich surface reaction layers with rising the pH. Positively charged Ca^{2+} interacts with the negatively charged PO_4^{3-} in the surrounding fluid provide the amorphous precursor for mineralization [13,14]. The amorphous calcium phosphate occurring in liquid phase change expansion cause the formation and crystallization carbonate hydroxyapatite [15].

Previous *in vitro* studies have proved that non-collagenous proteins (NPCs) play a crucial role in formation of healthy teeth, for instance, the regulation of crystal nucleation, control crystal shape, inhibition mineralization and stabilization metastable mineral phases [16,17]. Phosphophoryn (pp) with a unique functional domain of Ser-Asp repeats (SDrr), is able to bind to hydroxyapatite (HA) and benefit the precipitation of calcium phosphate [18]. The high charged N terminus of DMP1, created by the Asp residues, has been claimed to inhibit HAP formation and stabilized the amorphous phase [19]. Moreover, acidic amino acid immobilized on matrix provided a nucleation center and promote mineralization by attracting Ca^{2+} and PO_4^{3-} ions and increasing the local supersaturation [20,21]. Other studies suggested that the acidic amino acids could be adsorbed in the surface of HAP and regulate the growth types of crystals [22–24]. However, the interaction of mineralization inhibitors and modulators present in Asp *in vivo* remains unknown.

The propose of the study is to evaluate the effect of conditioning solutions containing amino acid on dentine under a simulated oral environment. Bioactive glass 45S5, as a remineralization material to occlude the dentinal tubules and a phosphate-containing and calcium-containing supplier, was applied in the present study as a remineralization medium.

2. Materials and methods

2.1. Dentine sample preparation

The study protocol of the experiment was approved by the local Ethics Committee of the School and Hospital of Stomatology Wuhan University, China. Thirty extracted non-carious human tooth were stored in 0.5% thymol (Sigma-Aldrich, St. Louis, MO, USA) at 4 °C no longer than a month prior to their use.

Sixty dentine discs with a thickness of 1.0 ± 0.1 mm were sectioned perpendicular along their long axes above the cemento-enamel junction using a low-speed water cooled diamond saw (Isomet, Buehler, Lake Bluff, IL, USA). The surrounding enamel of the disks was removed using tungsten air-rotor carbide burs under continuous water spray. To ensure a smooth surface on the specimen, all sections were manually polished the occlusal surface using silicon carbide grinding papers (Yuli Abrasive Belts, Shanghai, China) of grit 1000–4000 for 30 s under constant water irrigation. The 40 specimens were partially demineralized in 0.5 M EDTA solution (pH = 7.4) for 5 min to create 3–4 μm demineralized dentin layer, followed by rinsing with distilled water (DW) for 30 s.

Twenty discs were randomly selected and prefrozen in liquid nitrogen for 10 min, then reduced to a fine powder (mean particle size <50 μm) after sufficient grinding. After EDTA etching for 24 h, the demineralized dentin powder was rinsed by distilled water and centrifugation at 3000 rpm for 15 min to remove supernatant liquid. The centrifugated deposit was resuspended with phosphate buffered saline (pH = 7.4) three times to rinse away residual demineralizing solution.

2.2. Pre-treatment with Asp

The Asp pre-treatment was carried out by immersing dentine sections into 10 ml of 10 mmol/L DL-aspartic amino (Sigma,

[1] These two authors contributed equally to this paper.
[2] This author contributed to the original idea of this paper.

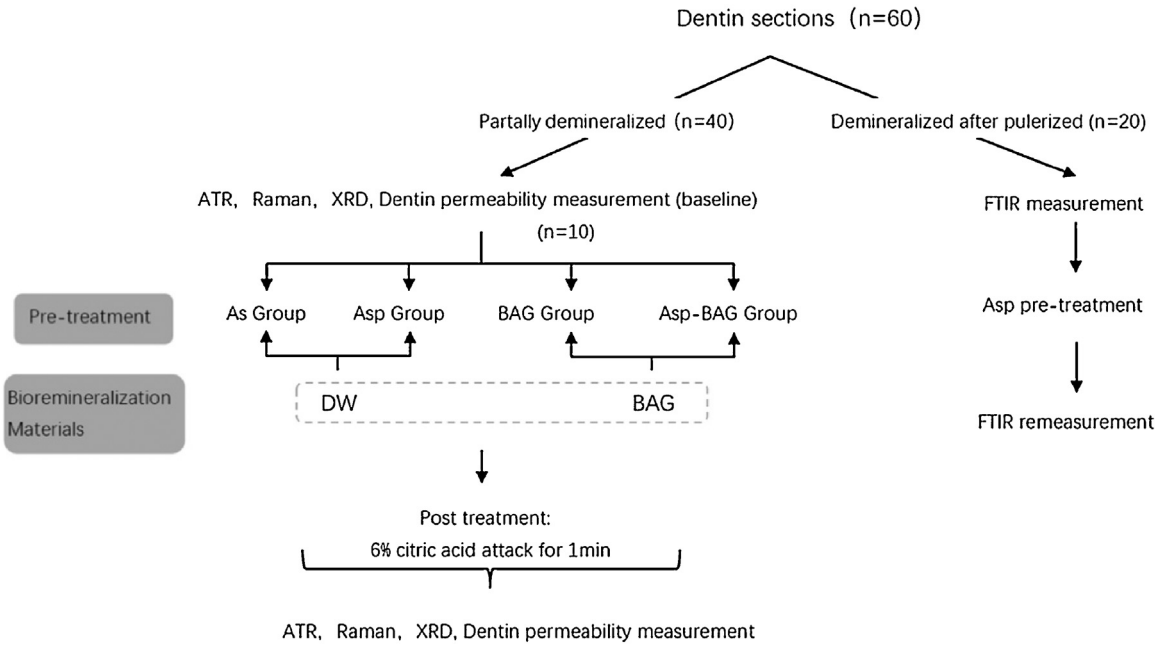

Fig. 1 – Experimental design in a simplified sequence flow diagram.

Chemical Co, USA) in a shaker at 37 °C for 30 min, followed by rinsing with distilled water and treating with DW or BAG.

2.3. *Experimental design*

Each disk was rinsed for the assessment of the maximum permeability, Raman spectra and ATR-IR spectra to collect the baseline data. The specimens were then divided randomly into 4 groups(n = 10):

AS (Artificial saliva) group: dentine disks pretreated and remineralized with DW as a control.

Asp group: dentine disks pretreated with Asp and remineralized with DW.

BAG group: dentine disks pretreated with DW and remineralized with BAG.

Asp-BAG group: dentine disks pretreated with Asp and remineralized with BAG.

The BAG suspensions particles (45 wt% SiO_2, 24.5 wt% CaO, 24.6 wt% Na_2O, 5.8 wt% P_2O_5, Osspray Ltd., London, UK) were mixed with deionized water with 1:1 in volume. The dentine surface in BAG group and Asp-BAG group was applied with a 2-mm thickness of bioactive glass using a cotton plier and wet cotton pellet for 5 min. After remineralization at room temperature for around 5 min, the residual BAG was rinsed by DW for 1 min. Dentine disks treat with AS (1.5 mmol/l $CaCl_2$, 50 mmol/l KCl, 0.9 mmol/l KH_2PO_4, 20 mmol/l Tris, Sigma-Aldrich, St. Louis, MO, USA) were chosen as control group to simulate oral environment. As in our pre-experiment or other *in vitro* studies, there was no statistical difference in different test methods between this formula of AS and distilled water [25,26]. All treated disks were stored in 50 ml AS for 7 days at 37 °C. And the solution should be changed 24 h with fresh AS. All of the four groups was treated with post-treatments with 6% citric acid (pH = 1.5) for 1 min to simulate eating or drinking something sour. Then samples were rinsed in distilled water. The experimental design was summarized in Fig. 1.

2.4. *Raman spectroscopy*

Raman spectra of same samples were recorded after EDTA etching and on day 1, 3, and 7 followed by acid challenge using a micro-Raman spectrometer (i-Raman Portable Raman Spectrometer, B&W TEK Inc., USA) equipped with a semiconductor laser diode at a 785 nm wavelength. Each specimen was analyzed in three points for averages using a 0–3200 cm^{-1} range and a 20,000 m s^{-1} integration time at room temperature. BWSpec 4 spectroscopic software (BWSpec, B&W TEK Inc.) was used to analyze the acquired spectra. Original spectra were baseline corrected and smoothed to avoid laser-induced fluorescence. Raman intensity (RI) at 960 cm^{-1} was calculated and all values were transformed to percentage values, where the changed values were calculated as a percentage of the baseline, compared in different times within and among groups.

2.5. *ATR-IR and FTIR analysis*

ATR-IR spectra of each groups were recorded after EDTA etching and on days 1,3 and 7 using a Nicolet 5700 FTIR spectrophotometer (Nicolet, Madison, WI, USA) equipped with a diamond crystal attenuated total reaction (ATR) accessory. Spectra were collected in the range from 800 to 1800 cm^{-1} at 4 cm^{-1} resolution, with 32-time scans. Each sample were completely air dried and measured at 3 different places for being averaged. The samples were fixed on the sample testing stage of ATR-FTIR, which will not alter their characteristics. Spectra of water was obtained and subtracted from each of the original spectra which were then processed by smoothing, baseline corrected, and normalized to the amide I peak.

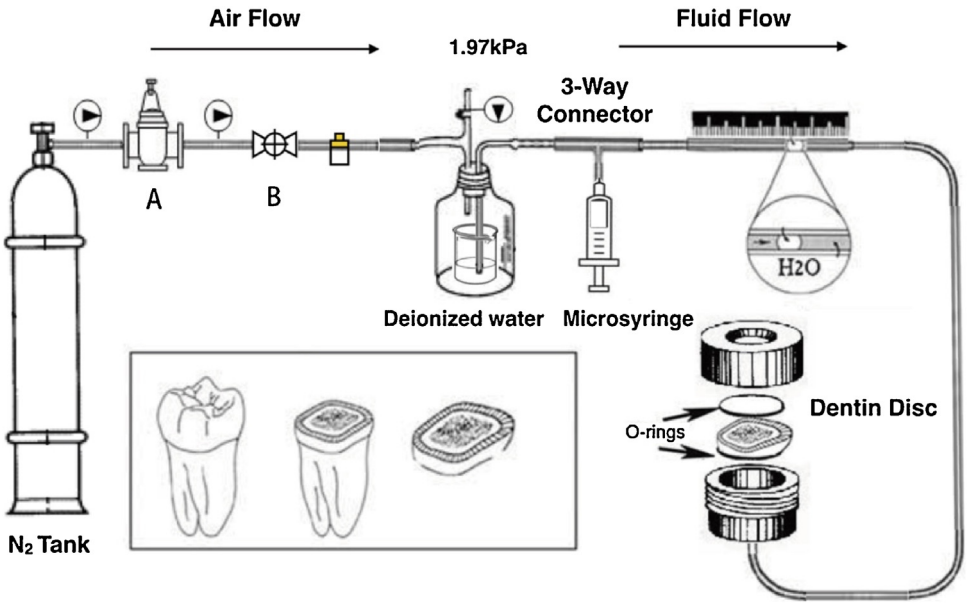

Fig. 2 – Dentine permeability device controlling nitrogen mobility through the gas pressure reducer(A) and quick release valve (B). Each dentine disk was placed between two O-rings and provided 0.282 cm^2 of available surface area for filtration of distilled water. Maximum permeability values were considered 100% of each specimen's filtration after EDTA etching.

The mineral matrix ratio (the ratio of integrated areas of the phosphate υ_1, υ_3 contour to the amide I peak) was measured in all spectra.

The dentine powders (50 mg) was immersed in 10 mmol/L Asp solution for 30 min, then centrifuged at 3000 rpm, filtered and air-dried. After mixing with potassium bromide powder, binding capacity of Asp to acid-etched dentine were measured with solid slice coupled with FTIR spectroscopy.

2.6. *SEM analysis*

Scanning electron microscopy (SEM) was used to observe the surface morphologies of the samples after treatment. The samples were sputter-coated with gold and examined using SEM (S-4800, Hitachi, Japan) using conditions of 20 kV at magnification ranging from 1500× to 8000×.

2.7. *Dentine permeability*

The dentine permeability of EDTA-etched dentin disks was quantitatively measured before and after the remineralization treatment in each group. The baseline permeability was recorded as the maximum permeability, which was assigned a value of 100% permeability. We used the device in Fig. 2 to measure the rate of fluid flow. The liquid propelling device provided a simulated pulpal pressure of 20 cm H_2O (1.97 kPa). When a steady-state of fluid flow is reached, the movement of an air bubble in a capillary tube along a scale was monitored for 5 min. The permeability of each specimen was expressed as a percentage (Lp%) of the fluid flow through the EDTA-etched dentine disc of the same specimen. Measurements were repeated 3 times to the 5 min intervals. Means (±SD) were obtained from the 3 measurements and the percentage relative to maximum permeability was calculated.

2.8. *XRD analysis*

X-ray diffraction (XRD) analysis was carried out before and after the 7-day remineralization in all groups by X'Pert PRO Dy2198 (Spectric Pte, Singapore) with a CuKa generator working at 40 kV and 40 mA. The range of scanning angles was from 208 to 558. The data were collected in the 2θ range of 20–40° at a scan rate of 2° per min.

2.9. *Statistical analysis*

Statistical analyses were performed with SPSS 19.0 (SPSS, Chicago, IL, USA). The repeated measures analysis of variance (ANOVA) was applied to evaluate the ATR-FTIR results Raman and dentin permeability among multiple groups, considering the treatment as main effect and treatment time as the repeated measure at a 5% significance level. Post hoc Tukey test was used to compare the difference within groups.

3. Result

3.1. *Raman spectroscopy*

Spectra of all specimens are dominated by the ν_1 phosphate (PO_4^{3-}) peak at 960 cm^{-1} were shown in Fig. 3. Phosphate peaks ratio of mineral peak at 960 cm^{-1} (phosphate) (PO_4^{3-}) before and after the 7-day remineralization were subjected to statistical analysis. Repeated measures ANOVA analysis revealed that a statistically significant main effect on the intensity of the υ_1 PO_4^{3-} value for both time and treatment and their interactions ($p < 0.001$). The intensity of υ_1 PO_4^{3-} slightly raised on after 7 days in AS group (0.99 ± 0.09) and Asp group (0.98 ± 0.05), but had no significant differences com-

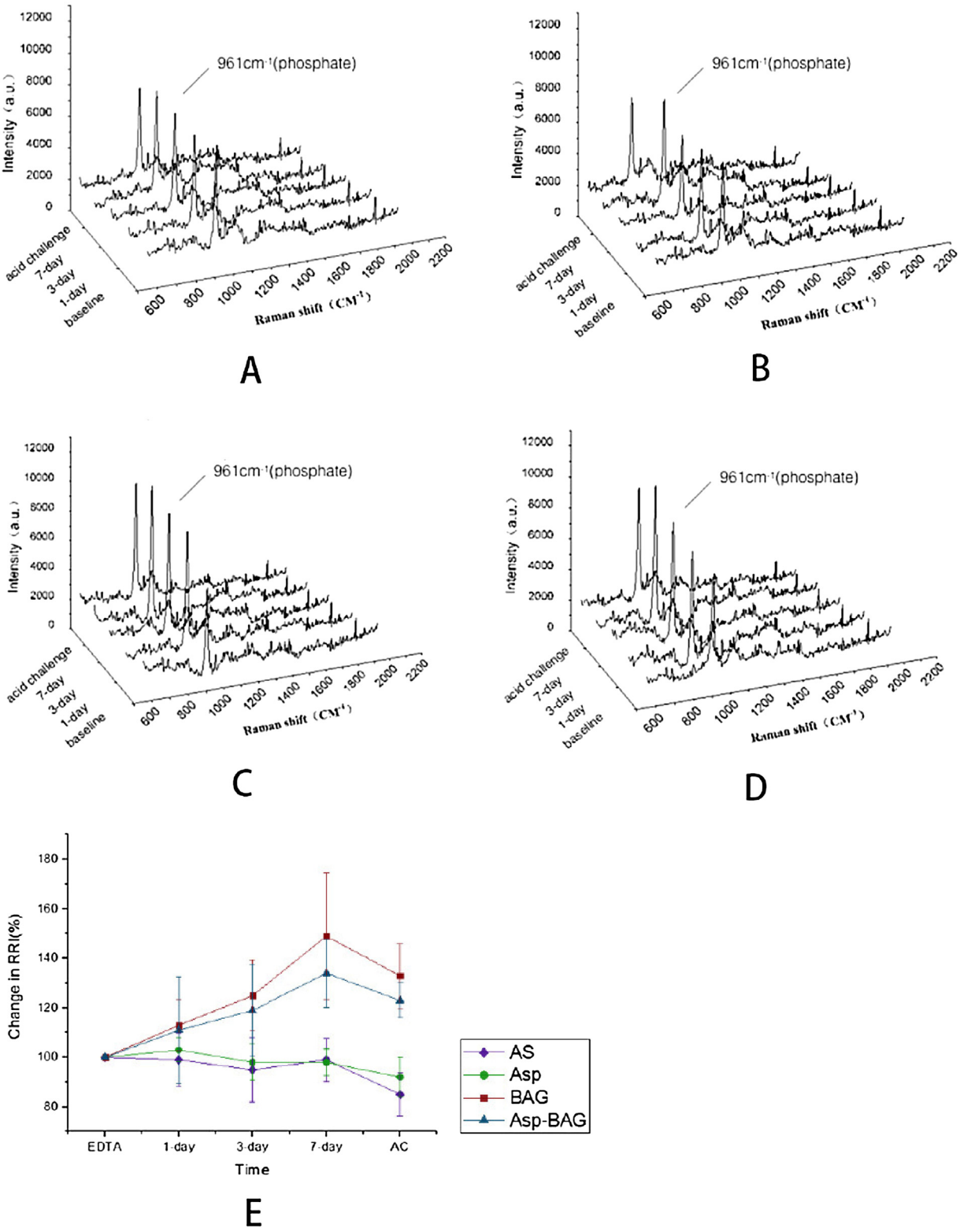

Fig. 3 – Raman spectra in fixed point of dentin surface remineralization marked in different colors at different time points. (A) AS group; (B) Asp group; (C) Asp-BAG group; (D) Asp-BAG group; (E) the ratio of intensity values of the v_1 PO_4^{3-} peak were recorded where the baseline ratio was set at 1.0 and the ratio that have been changed afterward were calculated as a relative ratio of the baseline.

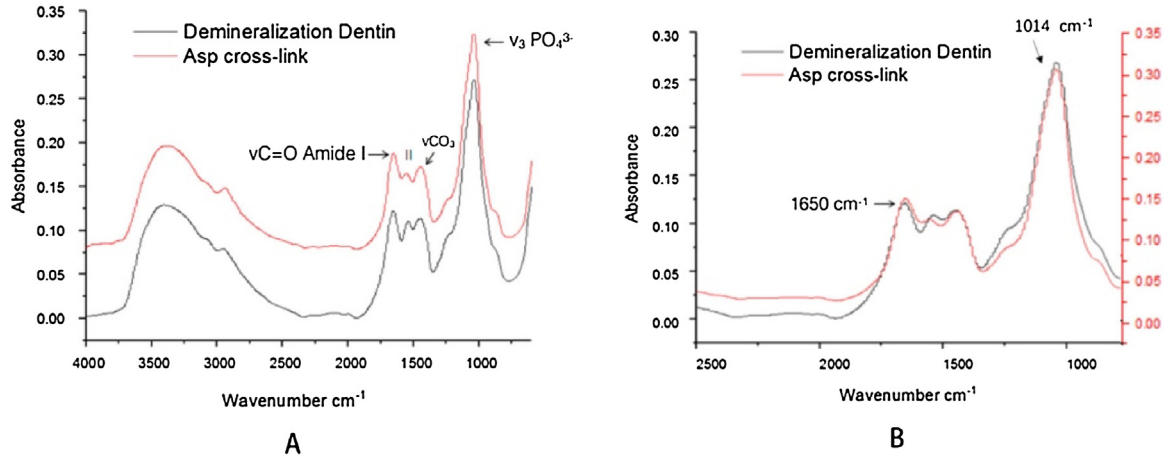

Fig. 4 – The ATR-FTIR spectra of partial demineralization dentine, EDTA etching dentin for 5 min (black line) and partial demineralized dentine treated with Asp (red line). Sharper amide bands were seen at 1650 cm^{-1} (amide I, C=O stretch), 1538 cm^{-1} (amide II, secondary N—H bond and C—N stretch), PO_4^{3-} absorption bands shows at 1014 cm^{-1}. (For interpretation of the references to colour in this figure legend, the reader is referred to the web version of this article.)

pared when after EDTA etching ($p > 0.05$). When the ratio after 1-day remineralization was compared with baseline values, there was no statistically significant difference between BAG group (1.13 ± 0.10) and Asp-BAG group (1.11 ± 0.22) ($p > 0.05$). However, the changes of Raman intensity (RI) in BAG group (1.49 ± 0.26) was significantly higher than that of Asp-BAG group (1.34 ± 0.14) ($p < 0.05$) after 7 days, and BAG group has the highest RI ($p < 0.05$) among these three remineralization materials. After facing an acidic environment for 1 min, there was no significance of the intensity of v_1 PO_4^{3-} in the AS and Asp groups ($p > 0.05$ and $p > 0.05$, respectively). But a significance reduction of the mineral matrix area ratio in the BAG group (1.43 ± 0.13) and Asp-BAG group (1.33 ± 0.07) was observed ($p < 0.01$, $p < 0.01$).

3.2. *ATR-IR and FTIR spectroscopy*

FTIR spectra of the demineralized dentin powers before and after immersing in Asp solution are shown in Fig. 4. After dentine was processed with EDTA, a clear presence of type I collagen (amide I and amide II bands) at 1650 and 1540 cm^{-1} as well as the phosphate group peaks at 1083 and 1034 cm^{-1} are weakened, indicating that the dentin was partially demineralized. The application of the biomimetic primers Asp solution increased the amide I and amide II bands. (Fig. 5)

Repeated-measures ANOVA and Tukey's multiple comparison tests illustrated a statistically significance main effect for both time and treatment and their interactions on the mineral matrix area ratio ($p < 0.05$). After 7-day remineralization process, the mineral matrix area ratio in AS Group (2.80 ± 0.87) and in the Asp group (4.38 ± 1.17), remained stable when compared with their initial values ($p > 0.05$ for both groups). Comparison between BAG group (2.84 ± 0.23) and Asp-BAG group (2.84 ± 0.63) revealed no significant difference after EDTA etch but significantly higher mineral matrix area ratio was found in BAG group (17.77 ± 2.27) than the Asp-BAG group (12.54 ± 2.29). After acidic challenge for 1 min, there was no significant change in the mineral matrix area ratio in the AS, Asp and BAG groups ($p > 0.05$). However, a significance decrease of the mineral matrix area ratio in the BAG-Asp group was observed ($p < 0.05$).

3.3. *SEM analysis*

After EDTA etching, partial demineralized samples were increased in the diameter of the dentinal tubules and hence formed a porous collagenous surface layer. After soaking in AS or Asp solutions without remineralization for 7 days, there was no change in the diameter of tubules (Fig. 6A–F). After dentine disks were remineralization by BAG with or without Asp pre-treatment after 7 days, the tubules were partially occluded, and the diameter of dentinal tubules became smaller (Fig. 6G–L).

After BAG contact dentine surface in liquid environment, BAG hydrolyzed and release calcium ions (Ca^{2+}) and phosphate ions (PO_4^{3-}) to from calcium phosphate rich surface reaction layers with increase of the pH. Positively charged Ca^{2+} interacts with the negatively charged PO_4^{3-} in the surrounding fluid provide the amorphous precursor to form apatite [13,14].

In the course of regulation of remineralization, the involved Asp includes two parts, dissolute form HA particle and diffuse out of college fiber. Due to BAG hydrolysis and pH rise, the absorbed amount of Asp decreased with an increase in pH [27]. In the meantime, the Asp monomer diffuse out of the gap zone and the calcium and phosphate ions reabsorbed back into the "recompressed sponge" by the force to balance electroneutrality and osmotic equilibrium simultaneously [28,29]. Other studies show that Asp was able to attach to the calcium phosphate-rich layer at the early stages of BAG surface reaction layer formation [30]. After the primary formation of hydroxyapatite crystals, the amino acids adsorb to sites on HA surfaces and blocking the active growth sites and slow the crystal growth rate, also result in the formation of two-dimensional plate-like crystals (Fig. 8) [22,24,31].

In Fig. 6I&L, adopting with the BAG agent, however, two kinds of typical appearances were observed. BAG group for-

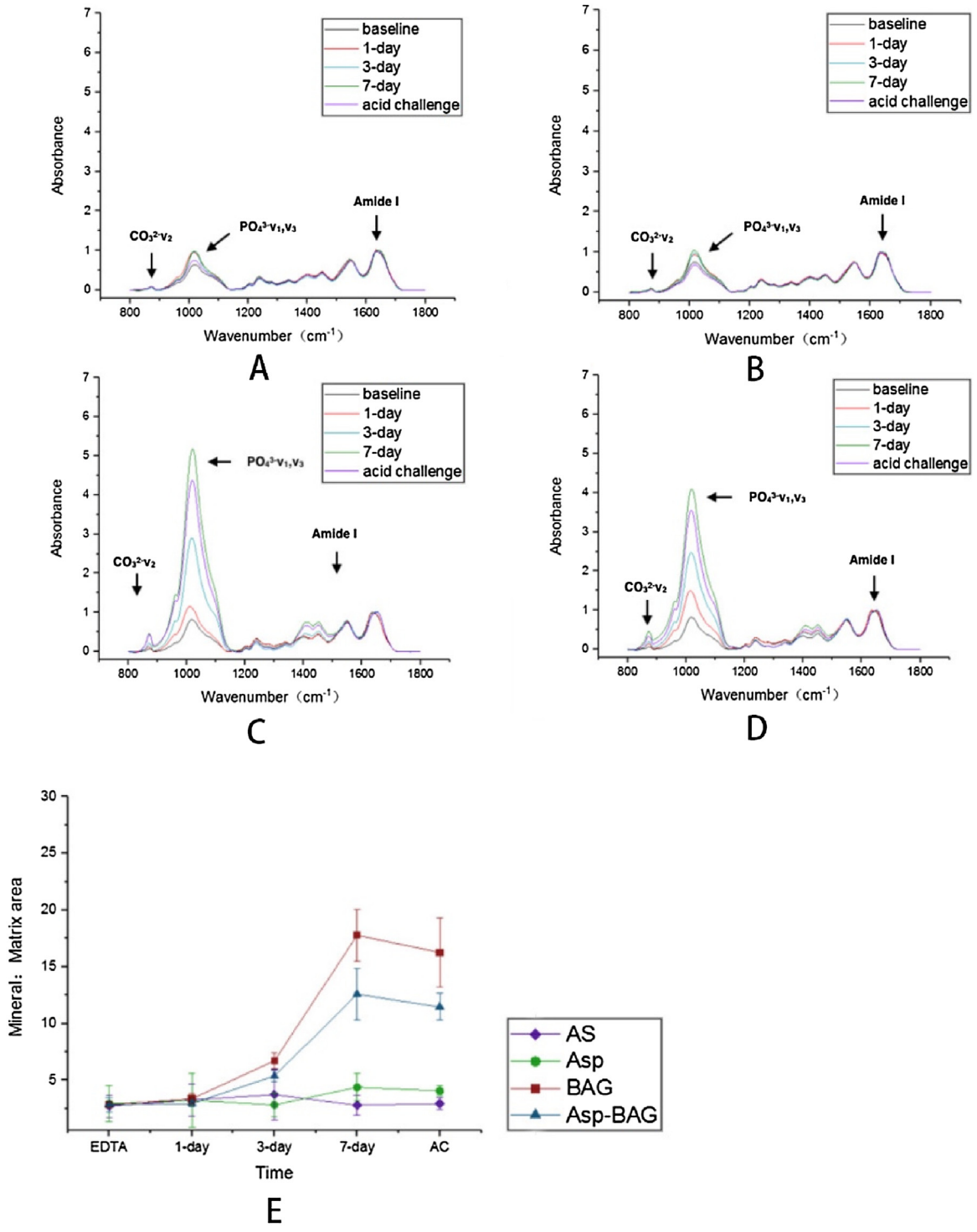

Fig. 5 – Representative ATR-IR spectra in fixed point of dentin remineralization marked in different colors at different time points. (A) AS group; (B) Asp group; (C) BAG group; (D) Asp-BAG group; (E) The mineral matrix area ratio after different time points for each group.

mation of rod-like crystals while the Asp-BAG group had large plate-like nanocrystals both covered the dentine surface. Fig. 6H&K showed dentinal tubules were occluded from the dentine surface to a depth of 6–10 μm. A thicker mineralized zone with granular crystallization was observed in Asp-BAG group comparing to flake-like crystals in BAG group. After acidic challenge (Fig. 7a–d), the dentine was re-exposed in AS and Asp group. However, the appearance and size of crystals in BAG (Fig. 7c) and Asp-BAG (Fig. 7d) groups remained unchanged.

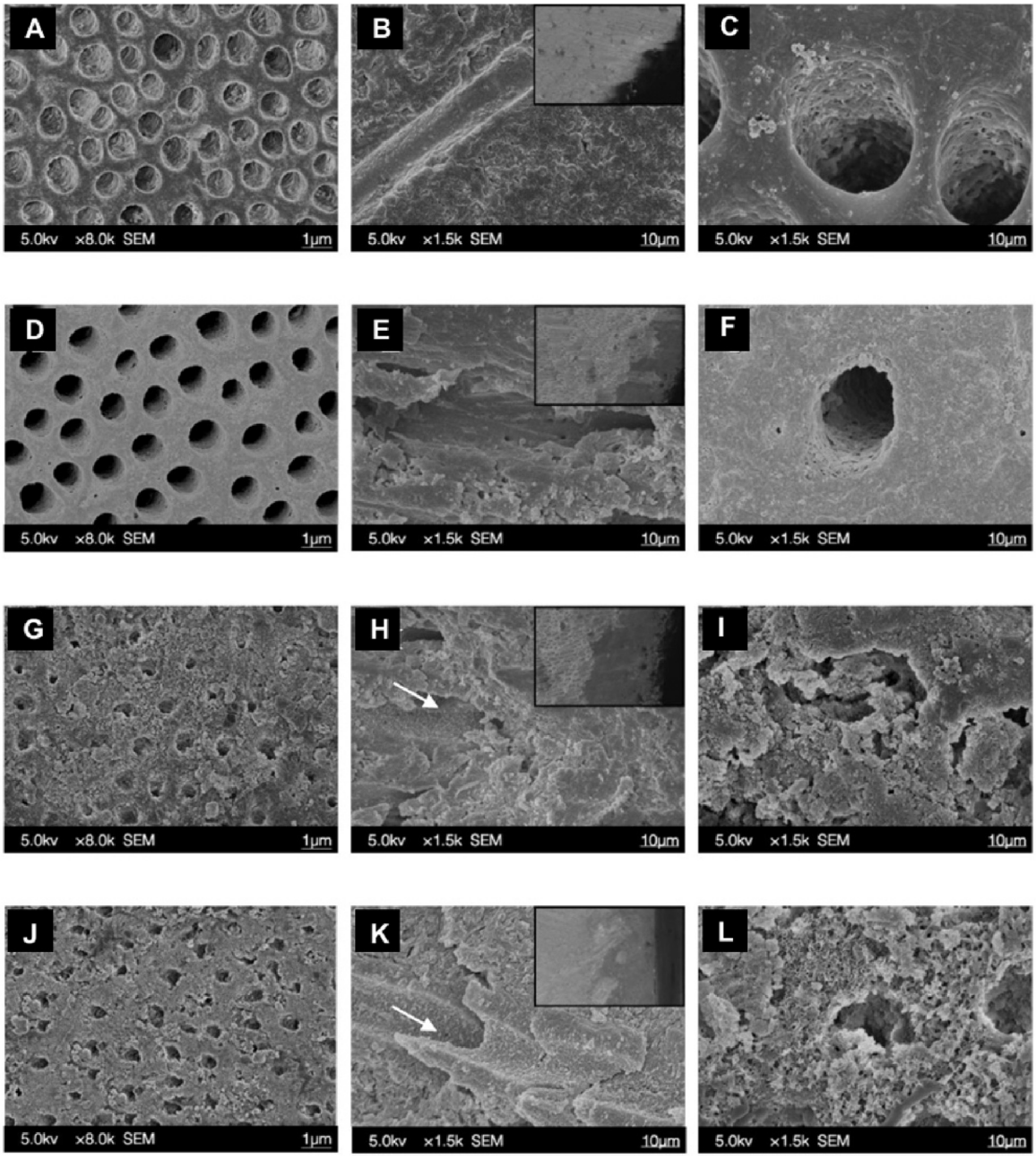

Fig. 6 – SEM micrographs of dentine surface and vertical cross-sections (middle column) morphology by different treatments after 7-day immersion and low(left column) and high (right column)magnification. The control sample in As group (A–C) the sample coated with Asp (D–F) the sample after remineralization using BAG (G, H) showing granular crystals (I) the sample pretreat with Asp after remineralization using BAG (J, K) showing petal-like crystals blocked the dentinal tubule (L). (H) and (K) showed the longitudinal section in BAG and Asp-BAG group. Remineralization particles precipitated along the inner wall of dentine tube (arrow).

3.4. *Dentine permeability measurements*

The dentine permeability results are expressed as percentages of the maximum permeability considered to be equal to 100% by EDTA etching. A repeated-measures ANOVA demonstrated statistically significant for the main effect of time ($p < 0.001$) and group ($p < 0.001$) Statistical analyses showed that the BAG group (30.0% ± 5.0%) and Asp-BAG group (41.0% ± 2.7%) significantly reduced the dentine permeability ($p < 0.05$), but AS group (93.0% ± 4.6%) or the Asp group (95.0% ± 5.2%) showed no statistically significant on dentine permeability ($p > 0.05$). After acidic challenge for 1 min, there was no significance change in dentine permeability in the AS, Asp groups ($p > 0.05$). A significant increase of the dentine permeability between the BAG and BAG-Asp groups was observed ($p < 0.05$) (Fig. 9).

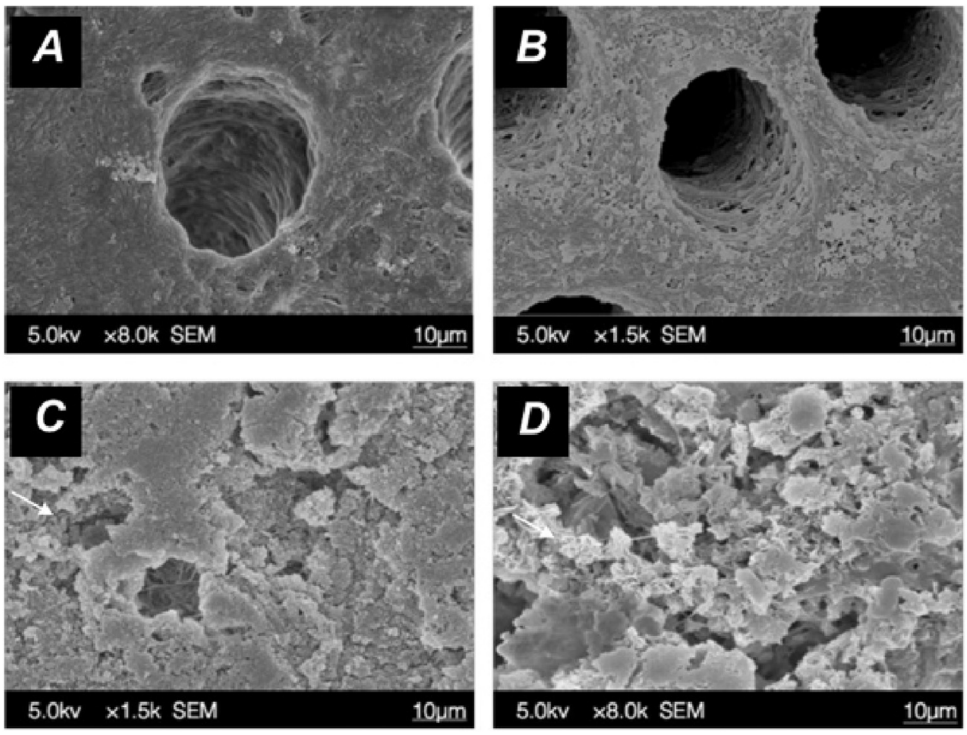

Fig. 7 – SEM micrographs of dentin surface at high magnification after acid etch. The sample in As group (A), Asp group (B), BAG group (C) and Asp-BAG group (D). The citric acid challenge caused more exposure of collagen fibrils in the dentine (A, B). The granular crystals (C) and petal-like crystals (D) blocked the dentinal tubules (arrow).

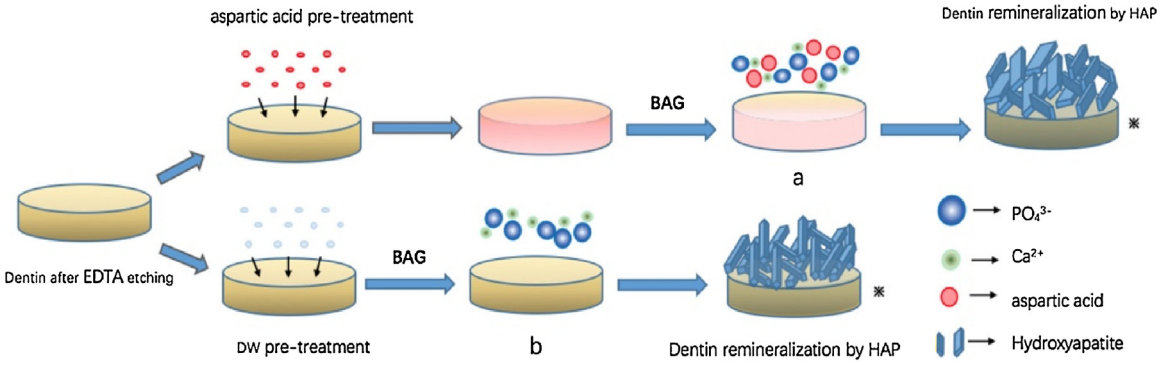

Fig. 8 – Schemas of remineralization process. (a) Hydroxyapatite formed in an Asp-rich environment. (b) Hydroxyapatite formed in an Asp-absent environment.

3.5. *XRD analysis*

Fig. 10 showed the XRD results of the surface of the dentine disks, before and after remineralization. The XRD pattern of the dentine disks in Groups C and D showed a main peak at around $2\theta = 32^{\circ}$ (211) and other typical peaks, which were matched the standard diffraction peaks of the hydroxyapatite (HAP) phase (JCPDS 09-0432), demonstrating that remineralization induces crystals that were predominantly composed of HAP.

4. Discussion

Aspartic acid was chosen as the amino acid used to regulate dentine mineralization in the present study. Aspartic acid is one of the necessary acidic amino acids in human body, which has been widely used in biochemical reagents [32,33] and can be obtained from dairy food and saliva [34]. Asp monomer has strong electronegativity in body fluids [35]. It has been reported that Asp amino can accelerate the crystallization kinetics of stabilized ACP and crystallization in gap zone within collagen fibrils [28,36]. Following the addition of amino acids, Asp monomer could inhibit crystallization and adsorb preferentially on specific faces of the growing crystals leading to a significant variation in crystal morphology [37–40]. With the addition of aspartic acid, Wu et al. reported the formation of carbonated hydroxyapatite crystals bundles was with more similar structure to human enamel [38]. In difference with the previous findings, in the present study, the initial seed crystal deposit randomly in irregular shape under the regula-

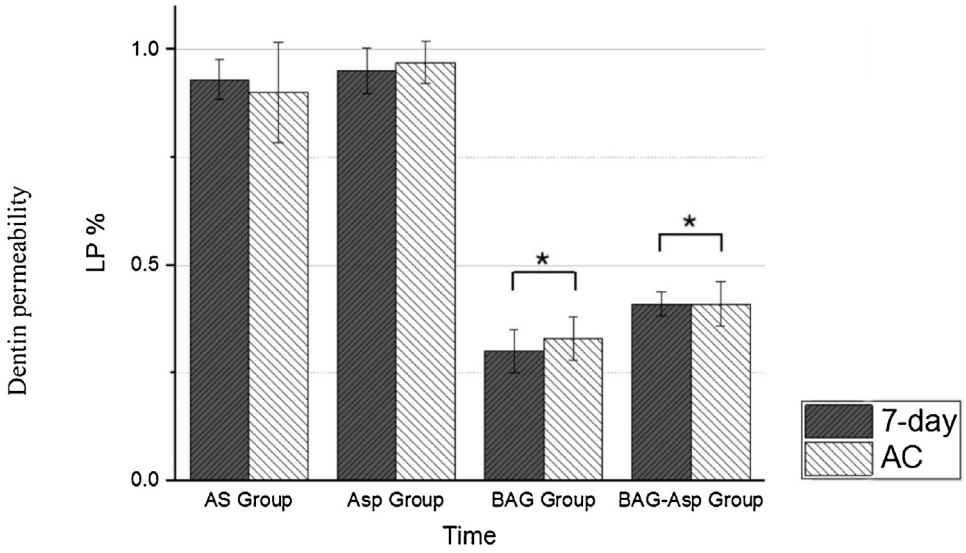

Fig. 9 – Dentine permeability after treatments and acid challenge.

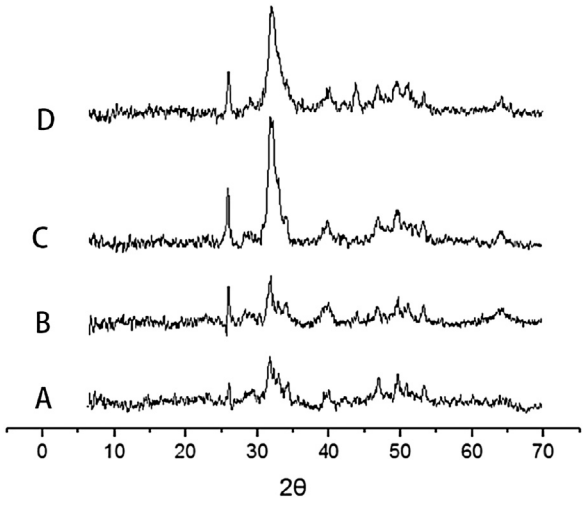

Fig. 10 – XRD patterns of samples as after 7 days. The sample in As group (A), Asp group (B), BAG group (C) and Asp-BAG group (D). The main crystal phase of crystal was hydroxyapatite (HA).

tion of Asp, resulting ina faster growth comparing to the BAG group.

Quantifying the changes of phosphate in Raman and the mineral matrix area ratio in ATR-IR reflects the crystallization formation on dentine surface. Both Raman and ATR-IR represented the dynamic characteristic of the degree of mineralization in real time [41,42]. Statistically significant difference ($p < 0.05$) was found after 7 days and changes of v_1 PO_4^{3-} in BAG is higher than the values in Asp-BAG group, which explains remineralization still took place in an aspartic-rich environment. After acidic challenging, a decreased mineral matrix area ratio and intensity of v_1 PO_4^{3-} in Asp-BAG group and a decreased intensity of v_1 PO_4^{3-} in BAG-promoting groups were observed. This result showed weakened crystals in apatite in the both BAG and Asp-BAG group after facing an acidic environment. Moreover, ATR and Raman spectra in Asp group showed that Asp did not interfere the remineralization process in a relatively high concentration of calcium and phosphorus environment. Since the high concentration of amorphous calcium phosphate environment, prompt HA precipitation influences more obviously on promoting remineralization than inhibitory effect caused by Asp [43]. This may explain how saliva contains certain amino acids and other proteins interaction with calcium and phosphorus ions.

Together with the quantitative spectral data from ATR-IR and Raman spectra, X-ray diffraction technique was used to confirm the formation of hydroxyapatite crystals, and no shift of the HAP peaks could be detected. In two BAG-promoting remineralization groups, minerals occluded dentinal tubules and dentin surface was covered by mineral crystals in SEM. Previous studies showed that the presence of the Asp occupy the vacant Ca and P sites of the growing HA (100) surfaces affected the surface structural order, regulate the growth and orientation in a direction parallel to the long axis of seed crystals [21,22,24]. This chemical surface modification may affect the HA biological properties and offer the potential for the nanocrystals to be used for optimizing the preparation of apatite as a biomaterial. Moreover, the possibility of tailoring the morphology of crystals and driving their assembly can help to understand how the classical shapes of crystals can be remarkably modified by biomolecules when formed by organisms.

The experimental equipment was used to simulate clinical conditions and assess hydraulic conductance after using mineralized materials. In previous experiments, variety of hydrostatic pressures were given to test hydraulic conductance [44–46]. The pressure gauge reading has to be kept at 1.5 kPa to simulate simulated pulpal pressure of 20 cm H_2O in physiological conditions [47]. In order to maintain stable transformation from gas pressure to fluid pressure, a quick release valve was used to prevent bubble compressive deformation by eliminate the residual air pressure. After 7-day remineralization, the dentine permeability result suggested

that the mineral crystals block dentine tubules effectively and may resist solubilizing by citric acid [17,48–50]. BAG has been proved to promote remineralization in non-classic way on mineral-depleted areas and increased nano-mechanical properties [51]. In the present study, the results suggested that BAG promoted hydroxyl apatite formation on partially demineralization dentin and block dentin tubule stability, which were resistant to solubilizing in AS or acidic environments. Aspartic amino bound to active growth sites of the crystal not only partially inhibit remineralization process but also regulate hydroxyapatite morphology. According to previous regeneration experiments, acidic amino with the HA structure enhances osteoblast activation and mineralization processes [23,52]. With understanding of the mechanism of bio-mineralization and regulatory organic molecule, we may have hard tissue restoration through a minimally invasive approach. Consequently, organic molecule regular inorganic mineralization has the guiding sense to the clinical treatment including teeth defect, secondary caries, and short durability of resin bonding.

5. Conclusions

This investigation confirmed the mineralization capacity of BAG. Asp could reduce the crystal growth rate and regulate crystal morphology. Understanding the role of Asp in mineralization process is helpful to further investigate the mechanism of in bio-remineralization.

Acknowledgment

This study was supported by the First Affiliated Hospital of Zhengzhou University (No.YNQN2017213).

REFERENCES

[1] Imbeni V, Kruzic JJ, Marshall GW, Marshall SJ, Ritchie RO. The dentin — enamel junction and the fracture of human teeth. Nat Mater 2005;4:229–32.
[2] Bleicher F, Richard B, Thivichon-Prince B, Farges J-C, Carrouel F. Odontoblasts and dentin formation; 2015. p. 379–95.
[3] Chu C, Lo EC. Dentin hypersensitivity: a review. Hong Kong Dent J 2010;7:15–22.
[4] West NX, Lussi A, Seong J, Hellwig E. Dentin hypersensitivity: pain mechanisms and aetiology of exposed cervical dentin. Clin Oral Investig 2013;17:9–19.
[5] Gillam DG. Management of dentin hypersensitivity. Curr Oral Health Rep 2015;2:87–94.
[6] Shiau HJ. Dentin hypersensitivity. J Evid Based Dent Pract 2012;12:220–8.
[7] Davari AR, Ataei E, Assarzadeh H. Dentin hypersensitivity: etiology, diagnosis and treatment; a literature review. J Dent 2013;14:136–45.
[8] Brännström M. The surface of sensitive dentine. An experimental study using replication. Odontol Revy 1965;16:293–9.
[9] Petersson LG. The role of fluoride in the preventive management of dentin hypersensitivity and root caries. Clin Oral Investig 2013;17(Suppl 1):63–71.
[10] Stoor P, Söderling E, Salonen JI. Antibacterial effects of a bioactive glass paste on oral microorganisms. Acta Odontol Scand 1998;56:161–5.
[11] Mehta D, Gowda V, Finger WJ, Sasaki K. Randomized, placebo-controlled study of the efficacy of a calcium phosphate containing paste on dentin hypersensitivity. Dent Mater 2015;31:1298–303.
[12] Palaniswamy UK, Prashar N, Kaushik M, Lakkam SR, Arya S, Pebbeti S. A comparative evaluation of remineralizing ability of bioactive glass and amorphous calcium phosphate casein phosphopeptide on early enamel lesion. Dent Res J 2016;13:297–302.
[13] Madan N, Madan N, Sharma V, Pardal D, Madan N. Tooth remineralization using bio-active glass — a novel approach. J Adv Dent Res 2011;2:64–7.
[14] Greenspan DC. NovaMin and tooth sensitivity — an overview. J Clin Dent 2010;21:61–5.
[15] Gorustovich AA, Roether JA, Boccaccini AR. Effect of bioactive glasses on angiogenesis: a review of in vitro and in vivo evidences. Tissue Eng B Rev 2010;16:199–207.
[16] Tay FR, Pashley DH. Biomimetic remineralization of resin-bonded acid-etched dentin. J Dent Res 2009;88:719–24.
[17] Niu LN, Zhang W, Pashley DH, Breschi L, Mao J, Chen JH, et al. Biomimetic remineralization of dentin. Dent Mater 2013;30:77–96.
[18] Baba O, Qin C, Brunn JC, Wygant JN, McIntyre BW, Butler WT. Colocalization of dentin matrix protein 1 and dentin sialoprotein at late stages of rat molar development. Matrix Biol 2004;23:371–9.
[19] Gajjeraman S, Narayanan K, Hao J, Qin C, George A. Matrix macromolecules in hard tissues control the nucleation and hierarchical assembly of hydroxyapatite. J Biol Chem 2006;282:1193–204.
[20] Zhu Z, Tong H, Jiang T, Shen X, Wan P, Hu J. Studies on induction of L-aspartic acid modified chitosan to crystal growth of the calcium phosphate in supersaturated calcification solution by quartz crystal microbalance. Biosens Bioelectron 2006;22:291–7.
[21] Matsumoto T, Okazaki M, Inoue M, Sasaki J, Hamada Y, Takahashi J. Role of acidic amino acid for regulating hydroxyapatite crystal growth. Dent Mater J 2006;25:360–4.
[22] Palazzo B, Walsh D, Iafisco M, Foresti E, Bertinetti L, Martra G, et al. Amino acid synergetic effect on structure, morphology and surface properties of biomimetic apatite nanocrystals. Acta Biomater 2009;5:1241–52.
[23] Boanini E, Torricelli P, Gazzano M, Giardino R, Bigi A. Nanocomposites of hydroxyapatite with aspartic acid and glutamic acid and their interaction with osteoblast-like cells. Biomaterials 2006;27:4428–33.
[24] Tavafoghi M, Cerruti M. The role of amino acids in hydroxyapatite mineralization. J R Soc Interface 2016;13(123).
[25] Sa Y, Gao Y, Wang M, Wang T, Feng X, Wang Z, et al. Bioactive calcium phosphate cement with excellent injectability, mineralization capacity and drug-delivery properties for dental biomimetic reconstruction and minimum intervention therapy. RSC Adv 2016;6:27349–59.
[26] Wang Z, Sa Y, Sauro S, Chen H, Xing W, Ma X, et al. Effect of desensitising toothpastes on dentinal tubule occlusion: a dentine permeability measurement and SEM in vitro study. J Dent 2010;38:400–10.
[27] Tanaka H, Miyajima K, Nakagaki M, Shimabayashi S. Interactions of aspartic acid, alanine and lysine with hydroxyapatite. Pharm Bull 1989;37:2897–901.
[28] Niu LN, Sang EJ, Kai J, Tonggu L, Mo L, Wang L, et al. Collagen intrafibrillar mineralization as a result of the balance between osmotic equilibrium and electroneutrality. Nat Mater 2017;16(3):370–8.

[29] Jiao K, Niu LN, Ma CF, Huang XQ, Pei DD, Luo T, et al. Collagen mineralization: complementarity and uncertainty in intrafibrillar mineralization of collagen (Adv. Funct. Mater. 38/2016). Adv Funct Mater 2016;26(38):6858–75.
[30] Mahmood TA, Davies JE. Incorporation of amino acids within the surface reactive layers of bioactive glass in vitro: an XPS study. J Mater Sci Mater Med 2000;11:19–23.
[31] Huang SP, Zhou KC, Zhi-You LI. Inhibition mechanism of aspartic acid on crystal growth of hydroxyapatite. Trans Nonferrous Met Soc China 2007;17:612–6.
[32] Ohzeki T, Machida S, Takahashi T, Ohtaka K, Kurosaka D. The effect of intravitreal N-methyl- DL-aspartic acid on the electroretinogram in Royal College of Surgeons Rats. Jpn J Ophthalmol 2007;51:165–74.
[33] Rajda C, Tajti J, Komoróczy R, Seres E, Klivényi P, Vécsei L. Amino acids in the saliva of patients with migraine. Headache 1999;39:644–9.
[34] Battistone GC, Burnett GW. The free amino acid composition of human saliva. Arch Oral Biol 1961;3:161–70.
[35] Kohlmeier M. Chapter 8 — amino acids and nitrogen compounds. In: Nutrient metabolism; 2015. p. 265–477.
[36] Sun J, Chen C, Pan H, Chen Y, Mao C, Wang W, et al. Biomimetic promotion of dentin remineralization using l-glutamic acid: inspiration from biomineralization proteins. J Mater Chem B 2014;2:4544.
[37] Wang Z, Xu Z, Zhao W, Sahai N. A potential mechanism for amino acid-controlled crystal growth of hydroxyapatite. J Mater Chem B 2015;3:9157–67.
[38] Wu X, Zhao X, Li Y, Yang T, Yan X, Wang K. In situ synthesis carbonated hydroxyapatite layers on enamel slices with acidic amino acids by a novel two-step method. Mater Sci Eng C Mater Biol Appl 2015;54:150–7.
[39] Yang X, Xie B, Wang L, Qin Y, Henneman ZJ, Nancollas GH. Influence of magnesium ions and amino acids on the nucleation and growth of hydroxyapatite. Crystengcomm 2011;13:1153–8.
[40] Koutsopoulos S, Dalas E. Hydroxyapatite crystallization in the presence of amino acids with uncharged polar side groups: glycine, cysteine, cystine, and glutamine. Langmuir 2001;17(4):1074–9.
[41] Yue S, Gao Y, Wang M, Wang T, Feng X, Wang Z, et al. Bioactive calcium phosphate cement with excellent injectability, mineralization capacity and drug-delivery properties for dental biomimetic reconstruction and minimum intervention therapy. RSC Adv 2016;6:27349–59.
[42] Wang Z, Jiang T, Sauro S, Wang Y, Thompson I, Watson TF, et al. Dentine remineralization induced by two bioactive glasses developed for air abrasion purposes. J Dent 2011;39:746–56.
[43] Rosseeva EV, Golovanova OA, Frank-Kamenetskaya OV. The influence of amino acids on the formation of nanocrystalline hydroxyapatite. Glass Phys Chem 2007;33:283–6.
[44] Vajrabhaya LO, Korsuwannawong S, Harnirattisai C, Teinchai C. Changes in the permeability and morphology of dentine surfaces after brushing with a Thai herbal toothpaste: a preliminary study. Eur J Dent 2016;10:239–44.
[45] Ishihata H, Kanehira M, Finger WJ, Shimauchi H, Komatsu M. Effects of applying glutaraldehyde-containing desensitizer formulations on reducing dentin permeability. J Dent Sci 2012;7:105–10.
[46] Ishihata H, Kanehira M, Finger WJ, Takahashi H, Tomita M, Sasaki K. Effect of two desensitizing agents on dentin permeability in vitro. J Appl Oral Sci 2017;25:34–41.
[47] Camps J, Giustiniani S, Dejou J, Franquin JC. Low versus high pressure for in vitro determination of hydraulic conductance of human dentine. Arch Oral Biol 1997;42:293–8.
[48] Kim J, Arola DD, Gu L, Kim YK, Mai S, Liu Y, et al. Functional biomimetic analogs help remineralize apatite-depleted demineralized resin-infiltrated dentin via a bottom-up approach. Acta Biomater 2010;6:2740–50.
[49] Sauro S, Osorio R, Watson TF, Toledano M. Influence of phosphoproteins' biomimetic analogs on remineralization of mineral-depleted resin-dentin interfaces created with ion-releasing resin-based systems. Dent Mater 2015;31:759–77.
[50] Liu Y, Mai S, Li N, Yiu CK, Mao J, Pashley DH, et al. Differences between top-down and bottom-up approaches in mineralizing thick, partially demineralized collagen scaffolds. Acta Biomater 2011;7:1742–51.
[51] Sauro S, Osorio R, Watson TF, Toledano M. Therapeutic effects of novel resin bonding systems containing bioactive glasses on mineral-depleted areas within the bonded-dentine interface. J Mater Sci Mater Med 2012;23:1521–32.
[52] Sarig S. Aspartic acid nucleates the apatite crystallites of bone: a hypothesis. Bone 2004;35:108–13.